Measurement of Microscopic Plastic-strain Distributions in the Region of a Crack Tip

Optical interference and moiré grid interference are used to measure plastic strains around a crack

by J. H. Underwood and D. P. Kendall

ABSTRACT—Two independent experimental techniques are used to measure the strain distribution within the plastically deformed region around a crack tip. Moiré grid interference is used to measure the in-plane strain with the specimen grid engraved directly on the specimen surface. Optical interference is used to measure the through-the-thickness strain over the same engraved area. The testing arrangement allows measurement of at-load strain as well as residual strain. The measured strain distribution is compared with recent work by Swedlow using a finite-element numerical technique and with results of the etch-pit technique used by Hahn and Rosenfield.

Introduction

When a sample of metal containing a crack or other similar defect is subjected to a tensile or shear stress, a very high stress concentration exists at the crack tip. If the material is assumed to remain elastic and the defect is sufficiently sharp, an analytical linear elastic solution for the stress and strain distribution in the region of the crack tip can generally be obtained. However, virtually all metals exhibit some ability to deform plastically without fracture. This results in a region of plastic deformation around the crack tip. If the size of this zone is very much smaller than all other significant dimensions of the structure and defect, the stress and strain distribution outside the plastic zone is not significantly different from the distribution predicted by the elastic solution. When the plastic zone becomes larger, as in a relatively ductile material, the applicability of the above concepts becomes questionable. Attempts have been made by Irwin[1] and others to correct for the effect of this plastic zone. These attempts have been somewhat empirical and approximate in nature, and, although they have been used with some success in predicting actual fracture criteria, they do not represent a true physical model of stress–strain condition at the crack tip.

In order to fully understand the complex problem of crack growth in ductile materials, either under quasi-static or fatigue loading, knowledge of the stress and strain distribution in the region of the crack tip is required. The factors required include such information as the size and shape of the plastic zone, the strain distribution within the plastic zone, and the effect of the plastic zone on the surrounding elastic stress distribution.

Analytical solutions to the above elastic–plastic boundary-value problem have been developed by investigators such as Rice,[2] and others. Most of these solutions have involved extensive simplifying assumptions or have used a physical model, such as anti-plane shear loading, which is not directly applicable to tensile-mode fracture of greatest practical interest. Recent work by Rice and Rosengren[3] and Hutchinson[4] applies directly to the tensile-mode crack problem. This work was reported in the literature during final preparation of this manuscript, thus no comparison with these results is shown here.

The crack-tip plasticity problem has also been studied using numerical techniques, such as the finite-element method. The most notable application of this method is that developed by Swedlow, Williams and Yang[5] and further developed theoretically by Swedlow.[6] The results of this work will be discussed in detail later. In the absence of a general analytical solution, an experimental technique is required to measure the strain distribution in the region of the crack tip on a microscopic scale.

In 1962, Oppel and Hill[7] published the results of a study evaluating the various techniques which could be used to conduct such an experiment. They indicated that the optical-interference technique provided the greatest sensitivity and accuracy. However, this method only provides a measurement of through-the-thickness strains in a sheet specimen. They discussed several other methods which could provide a means of measuring

J. H. Underwood and D. P. Kendall are Research Physical Metallurgist and Project Engineer, respectively, Maggs Research Center, Watervliet Arsenal, Watervliet, N. Y.

Paper was presented at 1968 SESA Spring Meeting held in Albany, N. Y., on May 7–10.

in-plane strains. The two which appeared to offer the best possibilities for this application were the photoelastic-coating method and the grid-interference or moiré method. The photoelastic-coating method has been used by Gerberich[8] to study crack-tip strains. It provides sufficient sensitivity for measurement of elastic strains and can also be used in the plastic region. It is relatively easy to use and does not require special equipment. However, it has two disadvantages which have caused the current authors to reject the method in favor of the moiré technique. Significant errors can exist in the photoelastic-coating method in regions of high strain gradients as pointed out by Duffy[9] due to the effects of the coating thickness and the resultant nonuniformity of strain through the coating. This method also prevents the simultaneous measurement of through-the-thickness and in-plane strains.

The moiré method has the advantages of being free from thickness-effect errors and being capable of measuring very large strains. If the specimen grid can be engraved directly on the specimen surface, there is no question as to the conformity of the grid with the surface. Also, the optical interference method can be combined with the moiré method to measure through-the-thickness strains directly on the ruled surface.

The disadvantages of the moiré method are the limited sensitivity and the fact that, since it is basically a displacement measuring method, it measures average strain over a finite "gage length." Both of these effects become less serious as the line spacing of the moiré grid is decreased. However, there is a practical limit to the line spacing which can be used and thus to the sensitivity of the moiré technique.

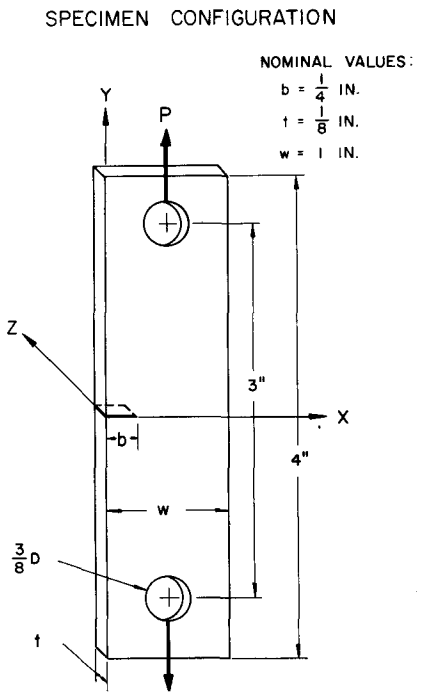

Fig. 1—Test-specimen configuration

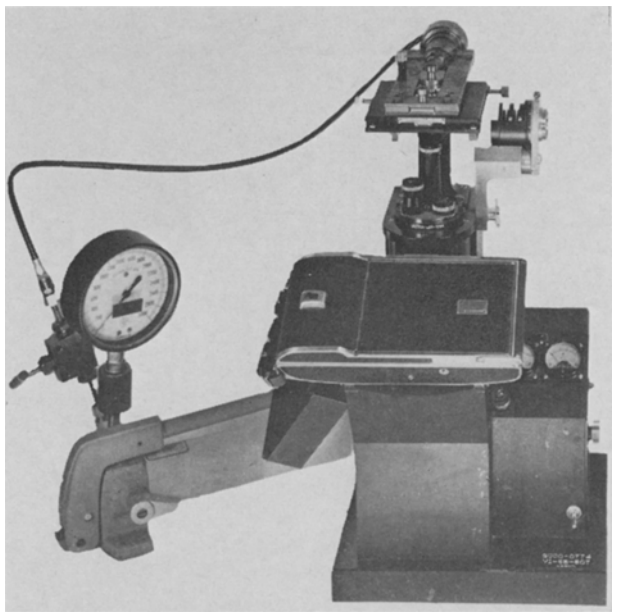

Fig. 2—Test equipment

The two techniques chosen to measure the strains around the notch are in reality surface-strain-measurement techniques; whereas the region of principal interest is the interior of the specimen in the area of the notch. Hahn and Rosenfield[10, 11] have developed and put to excellent use a method for directly measuring the interior strains in the area of a notch. By using the etch-pit response of 3-percent silicon iron to plastic strain, the shape of the plastic zone and, to some extent, the strains within the zone can be measured in the interior of the specimen as well as on the surface. Data obtained using the etch-pit technique on the surface and interior of a silicon-iron specimen will be compared with moiré and interference data taken from the same specimen.

In order to use surface-strain-measurement methods to determine the interior strains around a notch, the testing conditions must be arranged so as to insure that the measured surface strains represent the strains in the interior of the specimen. In this investigation, the specimen geometry and load values were chosen in an attempt to obtain this condition, as will be discussed later.

Experimental Methods

Specimen Preparation

The specimen configuration used in this investigation is a single-edge-notched sheet, pin loaded in tension, shown in Fig. 1. The specimens are relatively simple to prepare, particularly for forming and sharpening the notch and for polishing the surface around the notch. Also, this configuration facilitates the viewing of the specimen while under load as shown in Fig. 2. The material used thus far is commercially pure copper obtained in cold-rolled, $^1/_8$-in. sheet. Also, one specimen of silicon

TABLE 1—DIMENSIONS OF SPECIMENS

Specimen	Material	Width, W, in.	Thickness, t, in.	Crack length, b, in.
C-26	Cu	0.98	0.112	0.28
C-28	Cu	0.98	0.114	0.26
C-29	Cu	0.98	0.055	0.26
C-30	Cu	0.98	0.113	0.25
H-1	Fe—3% Si	1.00	0.121	0.25

iron has been tested for comparison. The exact dimensions for each of the specimens are listed in Table 1.

The notch length, b, is produced by cutting an initial notch with a 0.01-in. jeweler's saw to a depth of about 0.2 in. The notch is sharpened in the case of the copper samples by a slight indentation with a common razor blade. This assures that a single crack will form during subsequent fatigue loading. The notch is extended about 0.05 in. by zero-to-tension loading in a Sonntag fatigue machine. This produces a notch which is uniformly sharp for all specimens. A load of 6000 psi (based on uncracked area) for about 100,000 cycles is required for 0.05-in. crack growth in the copper specimens; a 16,000-psi load is required for the same conditions in the silicon-iron material.

The copper specimens are annealed following fatigue cracking to remove any effects of cold working resulting from machining and cracking. The annealing procedure is 1 hr at 480° C in argon atmosphere and it results in an average grain diameter of about 0.1 mm. The 0.1-percent yield stress measured from four tensile specimens of the same material and processing varied between 5830 and 6270 psi. The copper specimens are then wet ground using standard metallographic techniques and final polished with diamond abrasives to produce as flat a surface as possible. The area around the notch is generally held flat within about 20 μin., in the order of the wavelength of the monochromatic light used for optical interference. This prepares the surface for ruling of the moiré grid as described in detail later. The procedure for the silicon iron is similar except that the annealing process, 1 hr at 800° C in vacuum, follows polishing and ruling. This assures that any deformation associated with ruling will be annealed out and will not interfere with the etch pattern resulting from subsequent loading of the specimen. A possible difficulty with the procedure of annealing after ruling is that the specimen may change shape enough during annealing to deform the moiré ruling. However, the ruling itself provides an excellent measure of specimen deformation and no significant deformation has been observed.

Ruling Procedure

The grating used for the moiré strain measurement is ruled on the polished specimen in a manner somewhat similar to that of Douglas, *et al.*[12] A standard biological microtome (A. O. Spencer) has been modified for the ruling procedure. The specimen is clamped in the existing specimen vise mounted on the moving head of the microtome. A diamond point is mounted at the end of a cantilever spring which is attached to the microtome base. As the specimen is moved downward, it moves past the diamond point which scribes an individual line. A retraction mechanism has been added which pulls the diamond point away from the specimen during its upward motion. The advance mechanism of the microtome provides the desired line spacing. All of the specimens reported herein are ruled at line densities slightly under 6000 lines per inch (lpi).

Two problems were encountered in developing the ruling procedure. Considerable time was required to find the optimum combination of ruling pressure, diamond-support stiffness, and diamond-point geometry required for ruling at high line densities. The second problem involved the inherent errors present in all mechanisms which use a lead screw to produce small linear movements, as is the case for the microtome used. A cyclic error with a period equal to the pitch of the lead screw invariably appears. The effect of this error is essentially eliminated by adding an inclined plane to the microtome advance mechanism. This reduces the period of the error by a factor of about 10, so that it no longer interferes with the moiré technique.

After ruling, the specimens are lightly repolished with aluminum oxide to remove the excess deformed material between the ruled lines. There is a critical balance between the width of the line and the space between lines. The combination of ruling and repolishing must result in a line width adequate for moiré analysis, as well as enough space width to produce the reflectivity required for the interference measurements.

Strain-measurement Procedure

The specimens are installed in a frame mounted

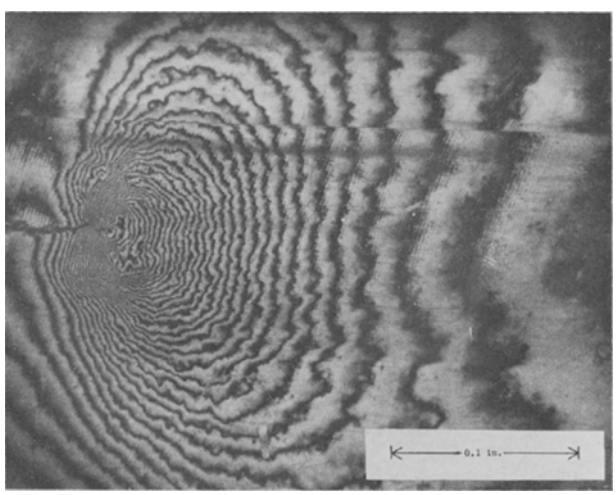

Fig. 3—Interference photograph. Specimen C-27; at $\sigma_A = 4780$ psi

on a standard metallurgical microscope equipped for low-power photography, shown in Fig. 2. The load is applied by a hydraulic cylinder so that either at-load or after-load photographs can be taken of the moiré and interference patterns. The load is measured by a precalibrated strain-gage load cell, pin connected to the specimen. The load-cell output is connected to a self-balancing digital strain indicator which continuously indicates the load on the specimen. The monochromatic light used to illuminate the specimen for the interference photographs is a thallium vapor lamp with a wavelength of 5350 Å. The standard white light supplied with the microscope is used for the moiré photographs.

The optical-interference fringe pattern is produced between the specimen surface and a glass proof plate held in contact with the surface. To increase the contrast of the fringes, a partially transparent layer of chromium is vapor deposited on the contact surface of the proof plate. The well-known condition for optical interference is used to measure the normal displacement of the surface relative to the proof plate. This displacement, denoted ΔZ, can be written in terms of the fringe order, n, and wavelength of light used for illumination, λ, as follows:

$$\Delta Z = \frac{n\lambda}{2} \tag{1}$$

If the Z-direction strain does not vary through the thickness, ϵ_Z is related to this displacement and the specimen thickness, t, by

$$\epsilon_Z = \frac{n\lambda}{t} \tag{2}$$

Any Z-direction strain which does not result in localized deformation around the crack tip will not be measured by the interference technique. The strains outside the crack-tip deformation zone are missed because the fringe order, n, in eq (2) is assigned the value zero for all points outside the zone. Therefore, all the Z-direction strain data presented herein are the sum of the strain calculated from eq (2) and a strain value which represents the uniform strain in the specimen away from the crack tip. The uniform strain used is that which would be obtained in an uncracked specimen for the same load and is in all cases less than 5 percent of the maximum strain measured ahead of the crack. This value is obtained directly from the uniaxial stress–strain properties of the specimen material in the same condition as the test material.

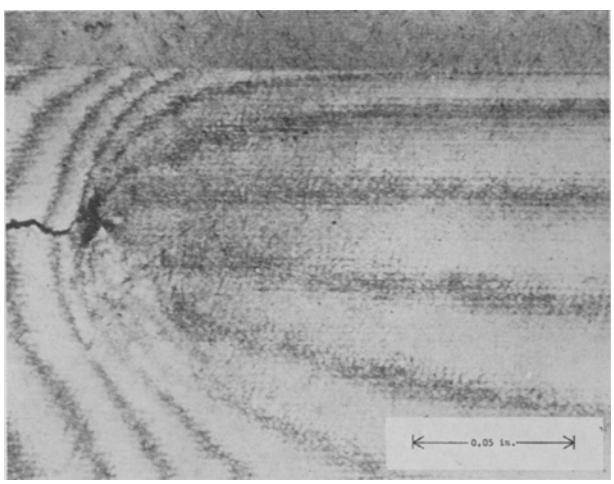

Fig. 4—Moiré photograph. Specimen C-28; after $\sigma_A = 5000$ psi

Moiré fringes are produced by placing a 2000-lpi master grating in contact with the specimen surface over the ruled area. Using specimen rulings of just under 6000 lpi, the fringes observed are the result of a third-order-diffraction effect. Thus, the analysis is the same as if a 6000-lpi master were used with the specimen grating, thus creating a slight mismatch between the gratings. Theocaris[13] has discussed differential-moiré strain analysis, i.e., moiré analysis with an initial mismatch between gratings. For measuring strains over small gage lengths with master gratings of slightly higher line density, as in this investigation, the following expression describes the Y-direction in-plane strain.

$$\epsilon_Y = \frac{\Delta V}{\Delta Y} - \alpha \tag{3}$$

where $\alpha = p/(d_o - p)$.

The α term is the mismatch constant and is determined as shown from the master grating pitch, p, and the no-load fringe spacing, d_o, resulting from the mismatch. The ΔV term can be thought of as the displacement of a point on the specimen which would cause a unit increase in fringe order; the ΔY term is the gage length over which the displacement occurs. For measuring average in-plane strain over a gage length of one fringe spacing, ΔV is equal to the master grating pitch and ΔY reduces to the distance between two fringes, d, resulting from the applied load. Equation (3) then becomes

$$\epsilon_Y = \frac{p}{d} - \alpha \tag{4}$$

The moiré strain-measurement technique described above applies only for the case of little or no rotation between master and specimen. If there is a significant angle between the grating lines of the master and the lines on the specimen, the analysis will be in error. Fortunately, the symmetry of the deformation about the line of the crack provides a sensitive method of aligning the master with respect to the specimen.

Results and Discussion

An optical-interference fringe pattern typical of those observed is shown in Fig. 3. The Z-direction strain corresponding to one fringe can be calculated from eq (2). For the $^1/_8$-in.-thick specimens and the 5350 Å light used, the value is approximately

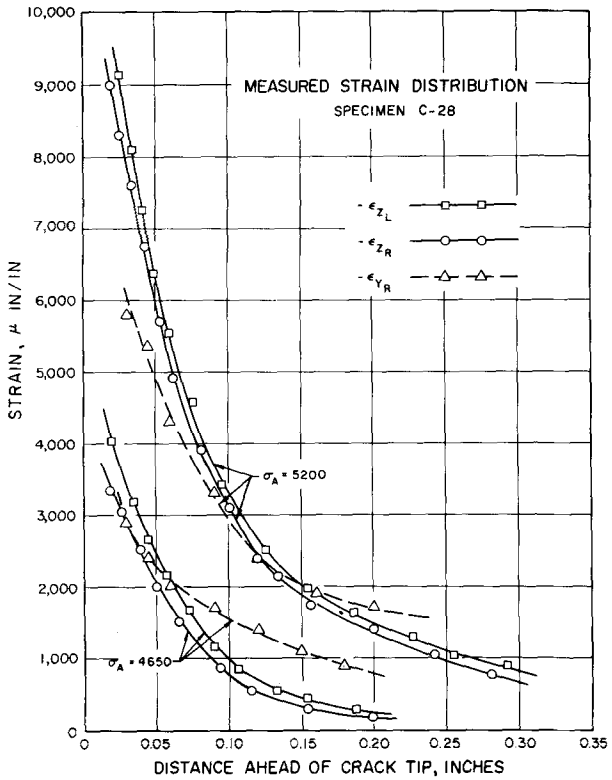

Fig. 5—Measured strain distribution for copper

180 μstrain/fringe order. The disturbance of the fringe pattern due to the ruled grating can be seen across the center on the photograph. In general, the pattern is shifted less than half of a fringe, so the indicated strain discontinuity due to the ruling is less than 100 μstrain.

It was stated in the "Introduction" that, in order to determine interior strains from surface measurements, the load and specimen geometry must be chosen correctly. The authors assume (1) that the condition required is that the loading should produce a deformation zone considerably larger than the specimen thickness, and (2) that a deformation zone which is large relative to thickness results in a uniform *Z*-direction strain through the thickness. The deformation zone described by the fringe pattern of Fig. 3 extends beyond the area of the photograph, about three times the specimen thickness in this case. For loads comparable to and higher than that of Fig. 3, the extent of the deformation zone in the copper specimens is a minimum of three times the thickness. Thus, the strain values reported herein are considered to be a good representation of the interior strain in the pecimen along the line ahead of the crack.

A photograph of the moiré-fringe pattern is shown in Fig. 4. The fatigue crack, opened somewhat as a result of loading, is clearly visible. The fringe spacing at the far right is slightly less than the no-load spacing which results from mismatch. The additional decrease in fringe spacing from right to left in the photograph indicates increasing strain in the *Y* direction (vertical direction). In the section describing strain measurement, eq (4) is used to calculate an average strain across a gage length of one fringe spacing. The fringes used to calculate the *Y*-direction strain ahead of the crack are the pair most nearly centered about the crack.

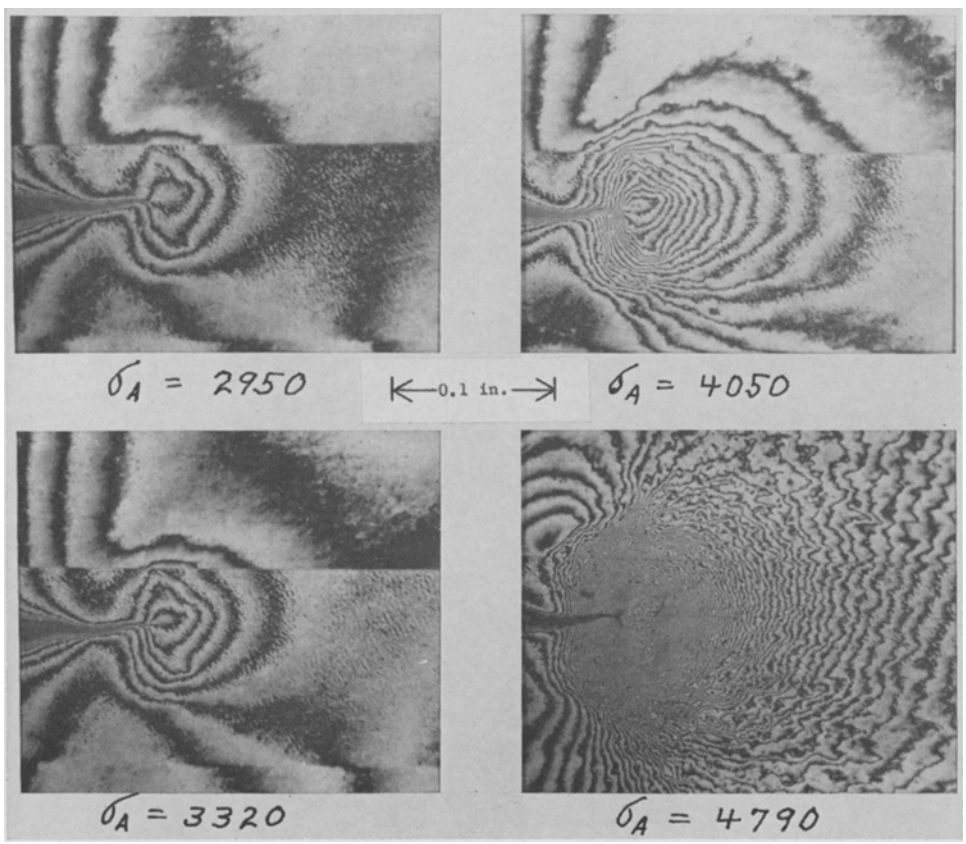

Fig. 6—Interference photographs for copper. Specimen C-26

If the Y-direction strain does not vary over a distance of at least one fringe spacing in the Y direction, then the measured average strain represents the actual value along the line ahead of the crack. An indication that the Y-direction strain is constant with Y is the fact that the spacings of the three central fringe pairs are nearly equal except very near the crack tip. Also, the interference patterns generally show (see Fig. 3) that the Z strain is constant with Y in the same area. Thus, the average strain calculated between the central fringe pair is reported as the value along the line ahead of the crack.

Figure 5 shows the strain distribution calculated from the interference and moiré photographs of specimen C-28 at two loads. The Z-direction strains are compressive, but have been plotted on the positive axis for ease of comparison. The general nature of the strain distributions shown is characteristic of all the copper specimens tested. The Z strains measured at load, ϵ_{ZL}, and after load, ϵ_{ZR}, are closely related for all specimens. The at-load strain is always slightly higher, as shown for specimen C-28, by an amount roughly equal to the Poisson strain calculated from the gross stress applied to the sample and the elastic properties. Also, in general, the magnitude of the Z strain is near that of the Y strain. Thus, if the X-direction strain is simply the algebraic sum of these strains, as predicted by the condition of constant volume, the strain value would be small. X strains were measured on one specimen and the results, although not conclusive, did indicate small positive X strain in the range from 0.05 to 0.15 in. ahead of the crack tip.

Figures 6 and 7 compare the after-load interference patterns from a copper and a silicon-iron specimen of the same size and geometry. Each figure shows a sequence of four photographs taken at loads arranged to produce approximately the same overall size of deformation zone. The difference in load required is primarily due to the difference in yield strength of the materials. The difference in the fringe pattern within the zone depends on the nature of the transition from elastic to plastic behavior of the two materials. The silicon iron, with the characteristic yield-point instability, exhibits a sharp transition from undeformed to deformed area, with a high concentration of fringes along the boundary of the deformation zone. The copper, which has a gradual transition to plastic behavior, exhibits a less clearly defined deformation zone.

After the final interference and moiré photographs were obtained from the silicon-iron specimen, it was sent to G. T. Hahn who measured the strains using an etch-pit technique. Photographs were taken of the surface etching pattern and also of the midsection pattern following sectioning and repolishing. The degree of etching response provides an approximate measure of the plastic strain in the deformed area. The complete details of the procedure are described in Refs. 10 and 11. The surface-interference photograph and the surface and midsection etch-pit photographs are shown in Fig. 8. There is excellent agreement between the overall extent of the surface-deformation zone as measured by the two techniques. The surface and midsection etch-pit patterns are quite different, thus indicating that the strains are not uniform through the thickness. Also, the width of the deformation zone is only 1.5 times the specimen thickness. Therefore, a quantitative comparison between strain determined using the two techniques cannot be made for the thickness (Z) direction. However, a comparison of Y-direction surface

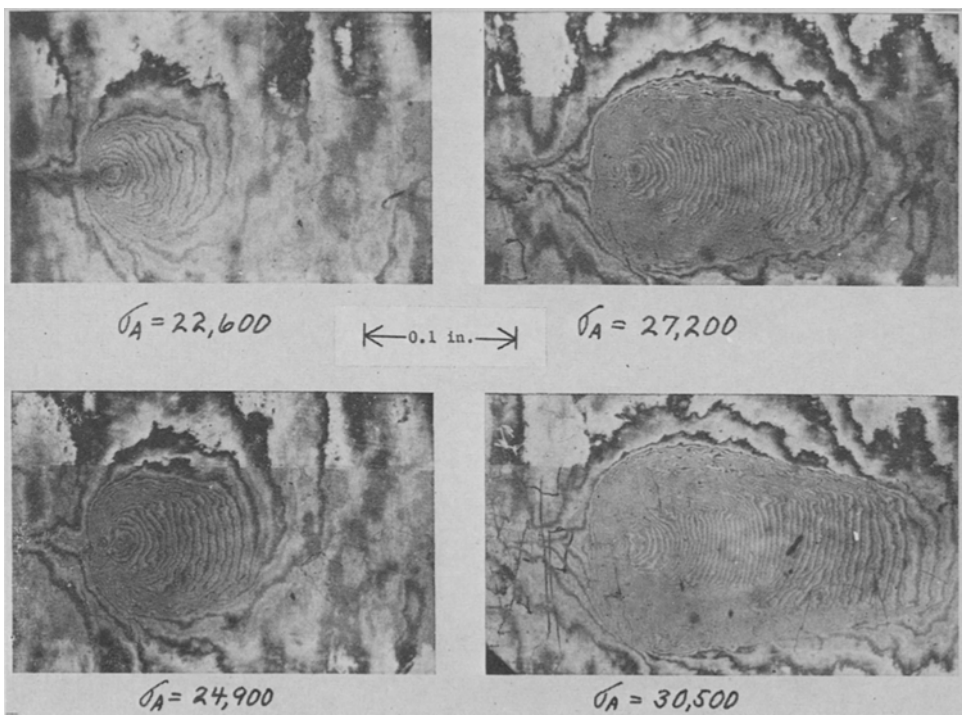

Fig. 7—Interference photographs for silicon iron. Specimen H-1

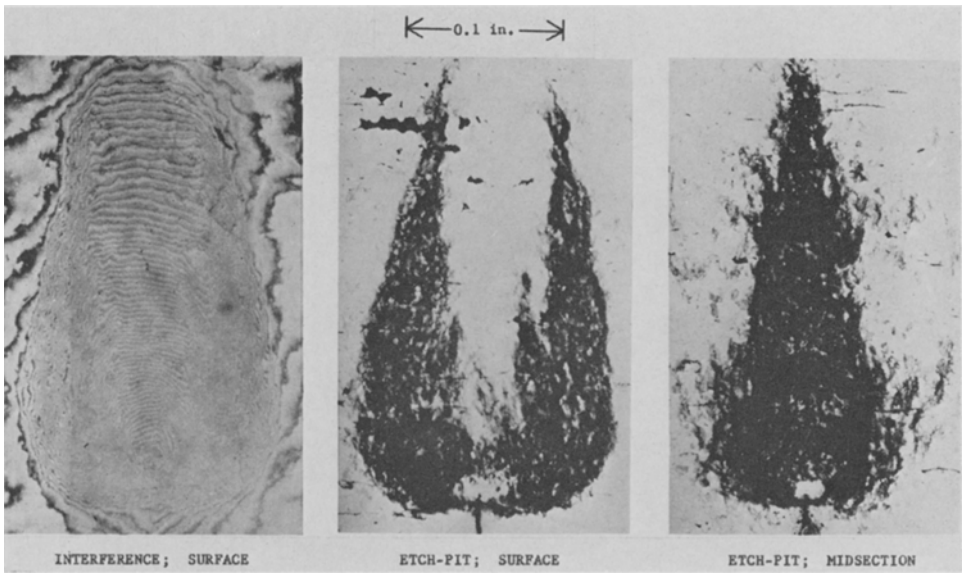

Fig. 8—Interference and etch patterns for silicon iron. Specimen H-1; after σ_A = 32,400 psi

strain measured by the moiré technique with that indicated by the etch-pit technique is appropriate, even with nonuniform strain through the thickness. The moiré data could be analyzed only in the widest portions of the two deformation bands shown in the surface etch-pit pattern. A strain of about 1 percent is calculated for the center of these bands at the two points about 0.03 in. ahead of the crack tip. This falls within the range of plastic strain predicted for these points by the etching response.

Strains measured by the interference and moiré techniques are compared with the results of some recent work by Swedlow.[14] He uses a finite-element technique[5, 6] in which the set of load–deflection equations corresponding to a triangular element array around the crack is solved by numerical methods on a computer. The uniaxial stress–strain data measured from the test material and the specific specimen geometry are used as input to the computer program. The complete two-dimensional stress and strain state is calculated by the program for both elastic and partially plastic loading. The boundary condition which simulates the specimen loading is a uniform tensile stress applied along the line 1 in. above the crack, i.e., along $Y = 1$. There was some question as to whether this loading produced the same elastic-stress field around the crack as does the pin loading of the test specimen at 1.5 in. above the crack. To answer this question, an 8/3-size photoelastic model of the specimen was prepared from Photolastic, Inc. Type PSM-1F material, with an f value of 37.0 psi/fringe/in. thickness. The results from the model test also served as an indication of the sensitivity and accuracy of the finite-element technique. The principal stress difference was cal-

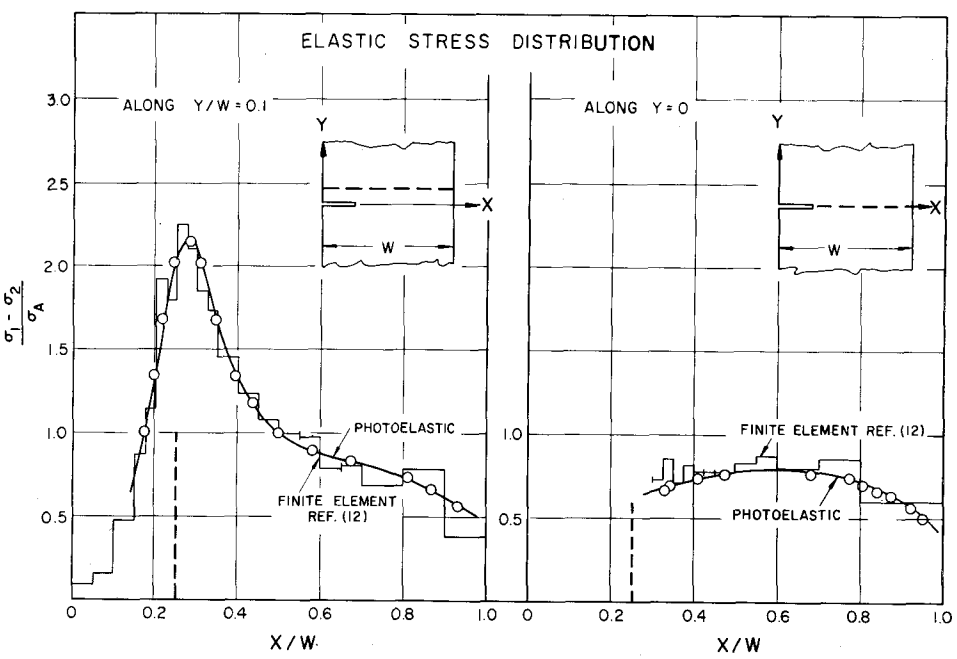

Fig. 9—Elastic stress distribution

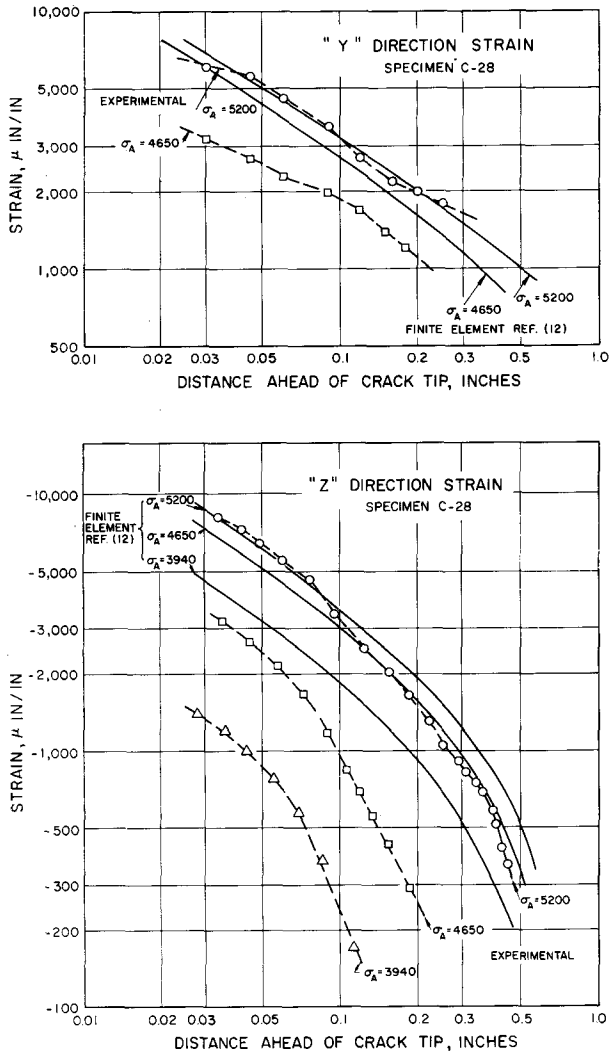

Fig. 10—Measured and calculated strain

culated from the photoelastic fringes along the line ahead of the crack and along a parallel line 0.1 W above the crack. These data are shown in Fig. 9. The finite-element results along the same line are shown as a stair-step plot where the width of each step indicates the size of the element at that location. The area of interest is along $Y = 0$, since most of the crack-tip data is measured along that line. However, the area above and below the crack is subjected to higher shear stresses, so a comparison of results along $Y/W = 0.1$ is a better check on the equivalency of loading condition. As shown, the pin loading of the test specimen results in very nearly the same stress distribution near the crack as that for the analytical model with a uniform load.

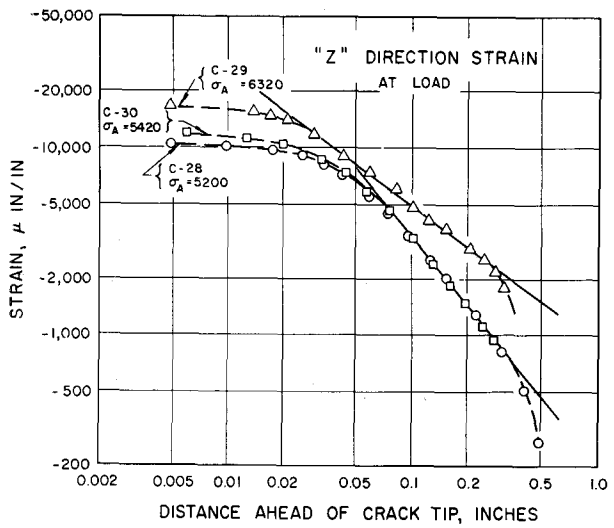

Fig. 11—Z-direction strain for three specimens

Both the measured strain distributions and those calculated by the finite-element method are shown as log-log plots in Fig. 10 for a typical copper specimen (C-28). At the highest load, very good agreement between the experimental and analytical results is obtained. However, at the lower loads, the measured strains are well below those predicted by the finite-element technique. This difference is believed to be due to the effect of Z-direction constraint imposed by the material outside the plastically deformed zone, particularly behind the crack tip. The effect of this constraint will increase as the size of the plastic zone decreases, so the larger difference between experimental and analytical results for lower loads can be explained. The constraint has the greatest effect on the Z-direction strains near the crack tip, as will be shown later, but indirectly affects the entire strain distribution. Since the finite-element technique is a two-dimensional analysis, it does not account for any Z-direction stresses which may develop. Thus, the finite-element technique yields significantly higher strain results for loads which result in plastic zones that are not large relative to the specimen thickness. A second factor which can contribute to the difference between analytical and experimental results is the uncertainty of the stress–strain data. If the data supplied for input to the analytical solution vary more than a few percent from the data which would represent the area around the crack tip, this could cause some of the difference noted above, particularly for the low-load data.

Another indication of constraint effects is shown in Fig. 11, a plot of at-load Z strains from three copper specimens. The area of deviation from the central linear portion of the data is believed to result from the Z-direction constraint described previously. The lower two curves, from full-thickness specimens, become nonlinear at about 0.06 in. ahead of the crack; the value for the upper curve, for a half-thickness specimen, is 0.03 in. Thus, for the material and specimen geometry used in this investigation, the area which directly shows the effects of through-the-thickness constraint appears to extend ahead of the crack tip a distance equal to about one-half of the specimen thickness. Further testing is required to determine the constraint effects in other specimen geometries and the extent to which material properties affect the significance of this constraint for any given geometry.

A field plot of the Z-direction strains at load for

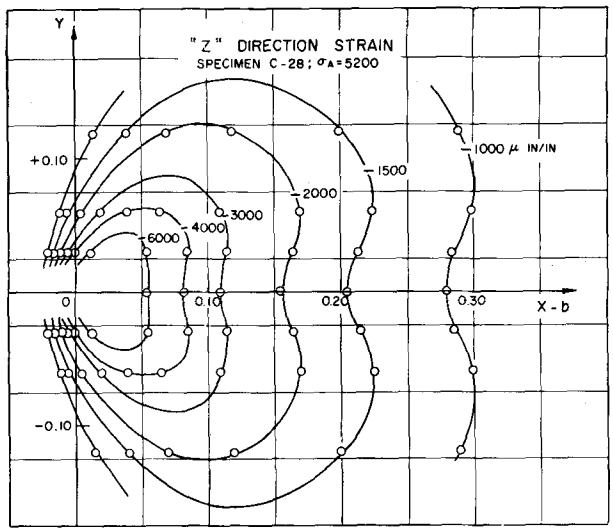

Fig. 12—Z-direction strain; field plot

specimen C-28 is shown in Fig. 12. The plot was constructed from data taken from an interference photograph along three parallel lines 0.03, 0.06 and 0.12 in. above the X axis in addition to the data directly ahead of the crack. As expected, the resulting pattern is similar in shape to a typical interference pattern (see Fig. 3). A field plot of Y-direction data is not presented since in much of the area immediately above and below the crack tip where the Y strain is greatest, significant rotation is also indicated (see Fig. 4). Thus, errors due to rotation would be present in the analysis of the moiré data as discussed previously. If the rotation errors were small, the full-field plot of the Y-direction strain resulting from typical moiré data would be generally similar to the Z-direction plot except in the region very near the crack tip.

Future work is planned to study in more detail the in-plane strains around a crack. Only slight modification of the current experimental technique is required to rule crossed gratings on the specimen surface. This would allow the measurement of in-plane shear strain and in-plane normal strain in two directions, while still maintaining the surface condition required for through-the-thickness strain measurement by interference.

Summary

Experimental methods have been developed to measure elastic and plastic strains on a microscopic scale in edge-cracked sheet specimens while under tensile load and after load removal. In-plane and through-the-thickness strains are measured on the specimen surface by moiré grid interference and optical interference, respectively. A 6000-lpi grating for moiré analysis is ruled directly on the specimen surface without affecting the interference results over the same area.

The strain distributions determined by the two techniques in copper specimens are nearly linear on a log-log plot, except for very near the crack tip and for low plastic strain. The through-the-thickness strain distribution deviates from linearity at a distance ahead of the crack equal to about one-half the specimen thickness.

Both the loading-direction and the thickness-direction strains measured in copper at relatively high loads agree well with those calculated by Swedlow's finite element solution of a similar model. For lower loads with small deformation zones ahead of the crack, the measured strains fall below those calculated by the finite element solution. The difference is attributed to through-the-thickness constraint which affects the experimental results, particularly for small deformation zones, but does not affect the finite element results since there is no thickness direction stress included in the analysis.

The extent of the deformed zone measured in a silicon-iron specimen by optical interference compares well with results obtained by G. T. Hahn using an etch-pit technique on the surface of the same specimen. A significantly different deformation zone was found at the specimen midsection using the etching technique.

Future work being planned includes crack-tip strain measurement in specimens with various stress–strain properties and thicknesses using optical interference and two-dimensional moiré analysis with crossed gratings.

Acknowledgment

The authors wish to express their appreciation to T. E. Davidson who conceived this research project and planned the initial stages. We also wish to acknowledge the help of W. Yaiser and D. Corrigan in conducting the experiments reported in this paper.

References

1. *Irwin, G. R., "Structural Aspects of Brittle Fracture," Appl. Matls. Res.,* **3,** *65 (April 1964).*

2. *Rice, J. R., "The Mechanics of Crack Tip Deformation and Extension by Fatigue," Brown Univ. Technical Report NSF GK-286/3 (May 1966).*

3. *Rice, J. R., and Rosengren, G. F., "Plane Strain Deformation Near a Crack Tip in a Power-Law Hardening Material," Jnl. Mech. Phys. Solids,* **16,** *1 (Jan. 1968).*

4. *Hutchinson, J. W., "Singular Behavior at the End of a Tensile Crack in a Hardening Material," Jnl. Mech. Phys. of Solids,* **16,** *13 (Jan. 1968).*

5. *Swedlow, J. L., Williams, M. L., and Yang, W. H., "Elasto-Plastic Stresses and Strains in Cracked Plates," Proc. First Internatl. Conf. on Fracture,* **1,** *259–282 (1965).*

6. *Swedlow, J. L., "Character of the Equations of Elasto-Plastic Flow in Three Independent Variables," Internatl. Jnl. Non-Linar Mech., to be published.*

7. *Oppel, G. U., and Hill, P. W., "Strain Measurement at the Root of Cracks and Notches,"* EXPERIMENTAL MECHANICS, **4,** *(6), 206 (1964).*

8. *Gerberich, W. W., "Plastic Strains and Energy Density in Cracked Plates, Part I—Experimental Technique and Results," Ibid.,* **4** *(11), 335 (1964).*

9. *Duffy, J., "Effects of the Thickness of Birefringent Coatings," Ibid.,* **1** *(3), 74 (1961).*

10. *Hahn, G. T., and Rosenfield, A. R., "Local Yielding and Extension of a Crack Under Plane Stress," Acta Metallurgica,* **13,** *293 (March 1965).*

11. *Rosenfield, A. R., Dai, P. K., and Hahn, G. T., "Crack Extension and Propagation Under Plane Stress," Proc. First Internatl. Conf. on Fracture,* **1,** *223 (1965).*

12. *Douglas, R. A., Akkoc, C., and Pugh, C. E., "Strain-field Investigations with Plane Diffraction Gratings,"* EXPERIMENTAL MECHANICS, **5** *(7), 233 (1965).*

13. *Theocaris, P. S., "The Moiré Method in Thermal Fields," Ibid.,* **4** *(8), 223 (1964).*

14. *Swedlow, J. L., private communication, work in progress under NASA Research Grant NGR-39-002-023. To be published in Internatl. Jnl. of Fracture Mechanics.*